1D/3D simulation procedure to investigate the potential of a lean burn hydrogen fuelled engine

1D/3D simulation procedure to investigate the potential of a lean burn hydrogen fuelled engine

Luigi Teodosio[1*], Fabio Berni[2], Alfredo Lanotte[1], Enrica Malfi[1]

1. Industrial Engineering Department, Via Claudio n.21, University of Naples, Federico II, Napoli, Italy;
2. University of Modena and Reggio Emilia, Via Pietro Vivarelli n. 10, Modena, Italy

*Corresponding author: luigi.teodosio@unina.it

Abstract. In recent years hydrogen, especially the one generated by renewable energy, is gaining increasing attention as a clean fuel to support the future mobility towards efficient and low emission solutions for propulsion systems. In this scenario, the present work deals with the virtual conversion of a single-cylinder Diesel engine, conceived for marine applications, into a hydrogen Spark Ignition (SI) unit. A simulation methodology is adopted, combining 1D and 3D Computational Fluid Dynamics (CFD) methods. First, experiments are realized on the original Diesel engine mounted on a test bench, collecting main performance indicators and emissions. A complete 1D engine model (GT-Power^{TM}) is developed and validated against measurements. Then, a 3D model of the cylinder (STAR-CD) is set-up and the related combustion outcomes are compared both with 1D and experimental results, showing an overall good agreement. In the second stage, the Diesel unit is converted into a port-injected hydrogen SI engine; the 3D model is re-arranged and utilized to reproduce pre-mixed hydrogen combustions under ultra-lean air/fuel (A/F) mixtures. Also, the 1D model is partly modified and coupled to an advanced combustion sub-model integrated with fast tabulated chemical kinetics to predict the knock. In particular, 1D combustion evolution is calibrated against the results of 3D CFD hydrogen combustion simulation. Finally, the calibrated 1D model is applied to investigate the advantages of ultra-lean hydrogen combustion in terms of efficiency, NO, and unburned H_2 formation at medium/high loads.

1. Introduction

In recent years, relevant attention has been posed to climate change due to greenhouse gas (GHG) emissions. To mitigate this issue, many efforts have been addressed at an international level towards the decarbonization process involving different energy sectors and including the transportation one. A more sustainable mobility can be not only achieved by the electrification of the powertrain but also through the development of alternative fuels capable to reduce GHG emissions. Among the available options, hydrogen is gaining increasing attention thanks to its capability to realize clean combustions and the possibility to be produced by renewable energy sources.
Hydrogen is already utilized in Fuel Cell (FC) applications, while the development of H_2-ICE is experiencing an increasing interest as a future option for clean powertrains. In this context, hydrogen fuel can be distributed utilizing the existing infrastructures, while hydrogen engines can be produced

by exploiting mature manufacturing facilities and procedures related to conventional engines, thus reducing the production costs.
In addition, the hydrogen's physical properties allow fast flame developments over wide ranges of pressure, temperature, and equivalence ratio. This involves the opportunity to realize a very lean mixture combined with optimal combustion phasing, which in turn enables high thermal efficiency and low cylinder-out nitrogen oxides (NOx), due to the low burning temperatures.
Although the hydrogen presents a high knock resistance [1], some issues may arise because of low minimum ignition energy [2], which strongly enhances the risk of pre-ignition or backfiring in the case of hydrogen port-injection. These aspects highlight the relevance of the design phase and the need to ensure the safe operation of hydrogen engines.
To this aim, many research projects have been carried out in recent years to deepen the efficient and safe development of hydrogen engines. Most of these research projects allowed the realization of engine prototypes for different applications [3], [4], identifying the powertrain configurations to achieve a good compromise between performance and costs.
A great variety of hydrogen applications based on different combustion concepts [5], [6] may be realized. A simple and effective solution is represented by the premixed SI combustion with the port hydrogen injection. Despite some drawbacks in terms of volumetric efficiency and the risk of backfiring, this configuration could be preferred for the newly produced H_2 engines to limit the manufacturer's costs.
An analysis of the literature papers highlights the presence of a limited number of experimental activities on hydrogen engines, probably due to the great efforts required in terms of time and costs and compliance with the safety protocols. As an example, Navale J.S. et al. [7] modified a single cylinder spark ignition engine to operate with hydrogen port injection, analyzing the engine behaviour at wide open throttle, maximum brake torque conditions, and low speeds. The hydrogen engine showed a peak of brake thermal efficiency improved by 3.16% with respect to the gasoline case. In addition, fast flame speeds, greater in-cylinder pressure peaks, and decreased NOx emissions (above 1700 rpm) were observed. A similar analysis was performed by Ganesh R.H. et al. [8]. They compared the performance at full load of a single cylinder engine running separately with hydrogen and gasoline. The hydrogen engine shows an increase in the brake thermal efficiency of 2% with respect to the gasoline one, thus confirming the outcome of the previous paper.
From the numerical point of view, some studies can be found in the literature on hydrogen SI engines and they mainly propose a methodological approach to evaluate and optimize the performance [9].
Keplatz. et al. [10] employed a 1D modelling approach, validated with a limited set of experiments related to the direct hydrogen injection realized into a donor Diesel engine. They explored injection timings and strategies, performing a thermodynamic losses analysis of the H_2-DI engine to compare the efficiencies of the direct-injected hydrogen engine with the ones of the Diesel unit. Scarcelli R. and Wallner T. [11], [12] developed a 3D CFD model of a single cylinder hydrogen unit, which was validated against the outcomes of an experimental activity performed on an optical access engine. The 3D model was adopted to analyze the effects of injector designs on air/hydrogen mixture formation and charge stratification. The result was the identification of a lean combustion system capable to achieve high indicated efficiencies (peak of 46-47%) while minimizing the NOx emissions penalty.
Also, Millo F. et al. [9] presented a synergic use of 0D/1D and 3D models to support the conversion of a 3.0 L Diesel engine into a hydrogen Spark Ignition one. The numerical optimization carried out on the engine allowed to achieve a peak of brake efficiency of about 41%.
In the light of the literature survey, the employment of reliable numerical tools and methodologies represents a fundamental step to properly forecasting the performance of a converted Diesel engine into a hydrogen-fueled engine and supporting its development stage with the availability of a limited data set.

To this aim, the present article proposes a numerical methodology capable to provide a first attempt estimation of the performance and emissions of a Diesel engine converted into a port-injected hydrogen Spark Ignition unit. In the first stage, the examined engine is briefly described in terms of

main characteristics and available experimental data. Then, the adopted models and the simulation methodology are deeply discussed. The latter is based on a hierarchical integration of 1D and 3D CFD codes applied to both the in-cylinder turbulence and combustion. 1D and 3D models are properly developed and validated against the measurements of the Diesel engine. Afterward, the original engine is virtually converted into a port-injected hydrogen Spark Ignition engine to numerically assess the performance variations; a 3D model of the cylinder is adopted to reproduce the in-cylinder turbulence level under motored conditions and, once properly re-arranged, it is also utilized to simulate a premixed hydrogen ultra-lean combustion. 3D outcomes are taken as a reference to calibrate 1D turbulence and combustion sub-models. In addition, the 1D model is further integrated with the refined knock and emission sub-models to detect the knock onset and to simulate the nitrogen oxides, respectively. In the last part of the article, the calibrated 1D model of a hydrogen engine is used to explore its potential at the same brake torque as the Diesel engine. The findings of this analysis in terms of performance and calibration variables are deeply discussed.

2. Engine system and experiments

The examined engine represents a single-cylinder Diesel unit conceived as a research engine for marine applications. The main characteristics of this engine are reported in the following Table 1. The cylinder is equipped with a centrally mounted 8-holes direct injector, providing Diesel fuel with a high injection pressure (1000 bar). A dedicated compression system is developed for the engine, which externally boosts the air to be delivered to the intake system. The engine is mounted at the test bench to perform steady state analysis and it is instrumented and interfaced with hardware/software systems for the data acquisition. In particular, the engine cylinder is equipped with a pressure transducer to detect the in-cylinder pressure traces. The engine is tested at high load operations and various speeds, acquiring the main performance variables (brake torque, air flow rate, fuel flow rate, boost pressure, etc.) and the in-cylinder pressure traces.

Table 1. Main engine features.

Engine Model	Single cylinder Diesel unit
Compression ratio	13.6:1
Bore/Stroke, mm	170/185
Displaced volume, cm^3	4200
Valve number	2 intake / 2 exhaust
Maximum brake power, kW	155 (@2100rpm)

3. Description of simulation methodology and models

A common approach in the field of numerical simulations for internal combustion engines is represented by the development of a 3D CFD model for a detailed analysis of single engine sub-components and the development of a complete 1D model for a system-level investigation to explore extensive operating conditions, up to the entire engine domain. Both 1D and 3D CFD models can profitably support the design of new engine configurations, thanks to the reasonable computational costs which can be realized with the actual CPU power. Moreover, these models can be combined to overcome their respective limits, thus creating a synergy of models. Indeed, the considered engine is studied following this approach, where the integrated 1D/3D numerical methodology is ultimately oriented to forecast the combustion evolution in the case of hydrogen operation. A 3D CFD model of the cylinder is built up and the related turbulence and combustion outcomes are utilized to calibrate predictive turbulence and combustion sub-models implemented into the 1D code. Knock tendency is

evaluated with the 1D approach employing a tabulated kinetic of ignition (TKI) method, providing the auto-ignition time of hydrogen/air mixture at varying operating conditions. A refined emission modelling is also considered to estimate the cylinder-out NOx and the unburned hydrogen quantity mainly arising from the crevice volumes. A deep description of the employed 3D and 1D models for the Diesel engine is presented in the following.

3.1. 3D model description

3D CFD in-cylinder simulation relies on a RANS approach to turbulence and is carried out by means of STAR-CD v2020 licensed by Siemens. The well-consolidated k-ε RNG model for compressible flows is adopted. Despite intrinsic limitations [13],[14], a high-Reynolds approach for the near-wall treatment is preferred to reduce the computational cost. In-house developed velocity and thermal wall functions which allow a grid-(that is y+-) independent result are used [15]. The GruMo-UniMORE heat transfer model is exploited to estimate gas-to-wall heat fluxes since widely validated in the past on Diesel engines [16],[17]. The computational domain includes the cylinder along with intake and exhaust ports. As for the mesh, the resulting total number of fluid cells is nearly 500 k at TDC and 1 M at BDC. Instantaneous boundary conditions in terms of pressure and temperatures are provided by a calibrated 1D model whose description is demanded in the following paragraph. As for the Diesel spray representation, atomization is replaced by a Rosin-Rammler distribution. The secondary break-up process is described via an in-house developed model, whose validation is reported in [18]. Senda's approach [19] is employed for droplet wall interaction. Liquid film modeling is accounted for (even if formation is almost negligible) and Habchi's model [20] is adopted for the estimation of the Leidenfrost temperature. Combustion is simulated by means of the ECFM-3Z [21] model, suitable for both premixed and diffusive combustion. As for flame quenching, the approach proposed by Bruneaux [22] allows accounting for thermal losses caused by the presence of cooled walls. Pre-ignition chemical kinetics is not on-line solved: auto-ignition delays are separately computed via the DARS solver licensed by Siemens and then stored in the table. Auto-ignition delays are computed by adopting a reduced mechanism from LLNL [23] describing the oxidation of a Diesel surrogate represented by an n-dodecane/p-xylene mixture. The same surrogate and mechanism are adopted to compute laminar flame speed values which are tabulated, similarly to ignition delays, as a function of unburned temperature, pressure, equivalence ratio, and EGR.

3.2. 1D model description

The engine is fully schematized in a commercial one-dimensional code (GT-Power). The developed engine model includes the network of intake and exhaust pipes, the cylinder with relative intake/exhaust valves, and the direct Diesel injector. According to the above-reported modelling approach, the unsteady 1D flow inside the intake and the exhaust sub-systems is solved, while the in-cylinder phenomena are simulated employing a 0D description. The flow permeability of the cylinder head is reproduced by the steady-state flow coefficients. Valve lifts and phasing are imposed as input variables in the intake/exhaust valve objects. Similarly, fuel injection strategy and injected Diesel mass per cycle are defined as input parameters, according to the experimental data. The turbocharger group is not modelled and the engine boosting is mimicked by controlling the plenum pressure. Referring to the in-cylinder processes (base Diesel engine), combustion, turbulence, and heat transfer are simulated through standard sub-models available in the commercial code. In particular, the premixed and diffusive phases of Diesel combustion are replicated by the 'DIJET' phenomenological sub-model. The latter is properly calibrated against the measurements and its parameters are left unchanged at varying the tested conditions. The Woschni-GT equation is utilized for the in-cylinder convective heat transfer. Referring to the 1D model set-up for the simulations, the input variables defined in the model are the engine revving speed, the injection timing, the injected Diesel mass per

cycle, and the fuel injection strategy; the boost pressure is automatically regulated by a PID controller to match the experimental air flow rate; the engine exhaust pressure, equal to ambient level, is also imposed as input.

4. Models validation

The reliability of 1D and 3D models is proved for the available experimental points through the assessment of the 1D/3D numerical outcomes with the measured counterparts.

In detail, the accuracy of the 1D/3D modelling approaches is tested both in terms of global performance parameters, NO emissions, and in-cylinder pressure traces. The main characteristics of the investigated points are resumed in Table 2, apart from λ which is different under Diesel operation. It is useful to highlight that the 3D analysis focuses on just one operating condition (1700 rpm), for computational cost reasons. Figure 1a depicts numerical/experimental comparisons of brake efficiency. Figure 1b reports a similar assessment for the NO emissions at 1700 rpm. On the numerical side, the presented NO values are the ones obtained in the cylinder just before the exhaust valve opening.

The proposed results demonstrate a good correlation of the models with respect to the experimental data in terms of efficiency and NO emissions. The prediction of the combustion process can be evaluated by the comparison of 1D/3D numerical and measured in-cylinder pressure cycles, as shown in Figure 1c for the point at 1700 rpm.

This figure confirms that the shape of the pressure profile is well captured by the developed 1D and 3D models. Although not reported here for brevity, also the engine brake torque is well predicted by the 1D model by imposing the air flow rate for the examined operating conditions. The presented figures underline that both simulation frameworks provide results close to their experimental counterparts.

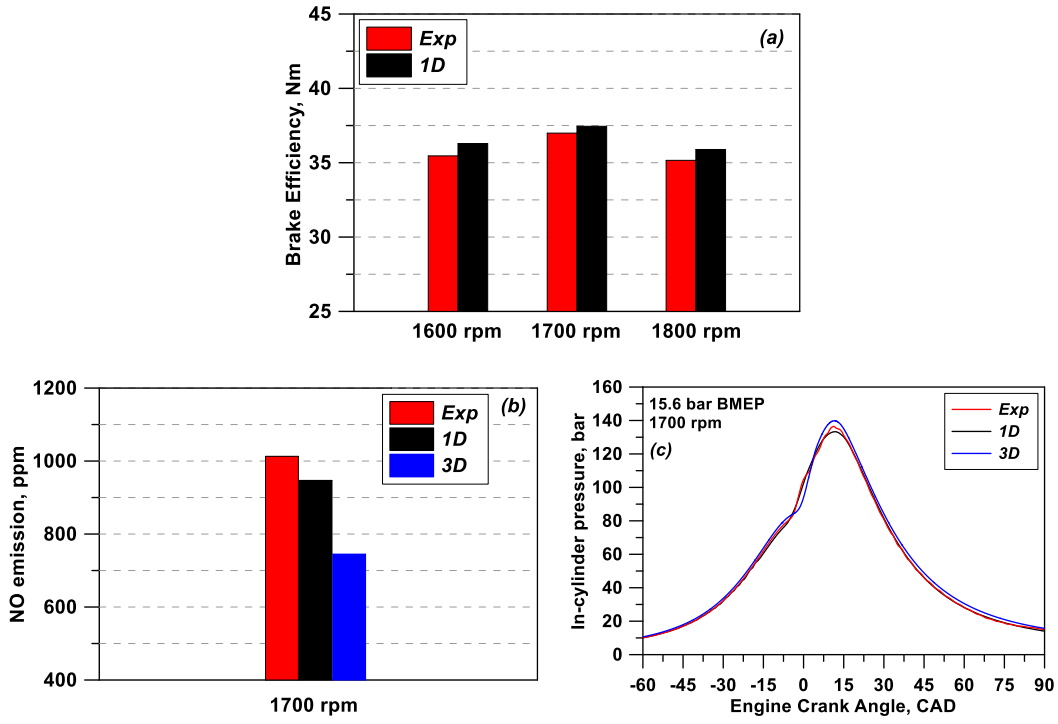

Figure 1. Numerical/experimental comparison of Brake efficiency (a); 1D/3D numerical/experimental comparison of NO emissions (b) and in-cylinder pressure cycle (c) at 1700 rpm.

5. Virtual conversion for port-injected hydrogen operations

The engine is virtually modified to study the potential of ultra-lean hydrogen combustion for performance improvements through port-injection configuration. To this aim, the adopted 3D and 1D models are re-arranged as deeply discussed hereafter.
The 1D/3D simulation methodology is applied to the converted hydrogen SI engine, performing two different 3D CFD analyses. The first one is conceived to derive the in-cylinder turbulence characteristics under motored operation at 1700 rpm, while the second one is represented by a combustion simulation realized at a high load point. These analyses furnish turbulence and combustion data to be considered as a reference for the tuning of the related 0D sub-models, implemented within the 1D code. Once properly calibrated against the 3D results, the 1D model is utilized in a predictive way to explore the benefits of ultra-lean hydrogen combustion for the examined engine, according to the operating conditions reported in the following Table 2.

Table 2. Test matrix.

Case	Label	Engine Speed, rpm	BMEP, bar	Relative air/fuel ratio, λ
Part Load	1800@17.4	1800	17.4	2.2
Part Load	1700@15.6	1700	15.6	2.2
Part Load	1600@13.4	1600	13.4	2.2

Simulations at part load are performed at the same experimental torque as the original Diesel engine, with an ultra-lean hydrogen/air mixture (relative air/fuel ratio, λ=2.2) and using a PID controller to match the load by adjusting the boost pressure.

5.1. 3D modelling

Since ECFM-3Z implemented in the adopted STAR-CD version does not support combustion simulation of hydrogen, it is replaced by G-Equation [24],[25]. The remaining aspects of the numerical framework are kept the same. G-Equation requires, as an input, a correlation for the turbulent flame speed. In the current analysis, the Peters correlation [24] is adopted, which is presented in [26] along with calibration constants. As for the laminar flame speed, the adopted correlation is shared with the 1D model and it will be extensively presented in the next paragraph. Two important aspects require ad-hoc modeling, namely knock and emissions. As for the former, the in-house developed knock model [27] is employed. It exploits the Livengood-Wu integral to predict knock onset, which in turn relies on ignition delays that are tabulated as a function of pressure, temperature, equivalence ratio, and EGR. Ignition delay calculation is carried out via DARS. Mauss chemical mechanism [28] is adopted, as validated in terms of ignition delays against experiments. As for the emissions, the Detail Chemistry model available in STAR-CD is activated in the burnt region. This allows incorporating detailed chemical kinetics calculations in that region (which is, in turn, delimited by the transport of G). The mechanism adopted for the Detail Chemistry model is still the one proposed by Mauss, as validated against experiments also in terms of NOx formation.

5.2. 1D modelling

Similarly, the 1D model of the original Diesel engine is converted to a Spark Ignition (SI) engine operating under an ultra-lean hydrogen/air mixture. In this context, a port hydrogen injector is virtually

mounted along the intake system, while the Diesel direct injector is replaced with a spark plug. The hydrogen is supplied by the port injector during the intake phase.
No geometrical modifications are virtually considered for the converted hydrogen SI engine, preserving the original cylinder/piston characteristics, and the intake/exhaust ports of the cylinder; also the valve strategies are kept the same as the donator Diesel engine.
Referring to the description of the in-cylinder processes, in-house developed sub-models of turbulence, combustion, knock, heat transfer, and emissions are implemented into the 1D code.
The in-cylinder turbulence evolution is reproduced by a 0D sub-model [29] which is demonstrated to adequately forecast the energy cascade mechanism from the macro-vortices to the micro-vortices. The turbulence sub-model is coupled to the combustion one. The latter is a predictive sub-model that can accurately simulate the combustion development in presence of limited experimental data or 3D CFD outcomes, as in the current study. The combustion sub-model is based on a physical background consisting of the fractal behaviour of a wrinkled flame front. Therefore, the model forecasts the enhancement of the flame front surface, relating the turbulent flame front extent to the laminar one through the turbulence characteristics [30]. Based on this approach, the burning rate is evaluated according to Equation (1):

$$\frac{dm_b}{dt} = \rho_u \cdot S_L \cdot A_L \cdot \Sigma \qquad (1)$$

where m_b is the burned mass, ρ_u the unburned gas density, A_L the area of the laminar flame front and Σ is the wrinkling ratio which accounts for the increased area of the turbulent flame front with respect to the laminar one, due to the turbulence. S_L represents the laminar flame speed of the considered fuel. In this work, a numerical correlation is adopted for the hydrogen, deriving from the fitting of chemical-derived laminar flame speed (LFS) computations realized under engine-like conditions (including the high load ones) carried out in DARS v4.3, licensed by Siemens, and using the reaction mechanism developed in [31]. The here employed LFS correlation presents the classical power-law formulation (Equation 2) [32]:

$$S_L = S_{L0} \cdot \left(\frac{T_u}{T_{ref}}\right)^{\alpha} \cdot \left(\frac{p}{p_{ref}}\right)^{\beta} \cdot EGR_{factor} \qquad (2)$$

As shown by Equation (2), the LFS is a function of the in-cylinder thermodynamic state (pressure and unburned temperature), mixture quality, and residual content. More details on the H_2 LFS correlation are reported in the reference [33], which includes all the fitting coefficients for the correlation along with the reference conditions and the range of validity.
Knock is modelled following a tabulated approach [34], considering the auto-ignition (AI) time of the unburned hydrogen/air mixture (end-gas). For knock computation purposes, auto-ignition tabulation is performed by simulations of the auto-ignition process in a homogeneous reactor for various initial conditions: pressure, temperature, equivalence ratio, and residual content. A progress variable expressing the variation of formation enthalpy of chemical species is considered, while the kinetic mechanism proposed by Hong [35] is employed for chemistry tabulation.
Table 3 reports the range and the step size of individual independent variables for the generated AI table.

Table 3. Variables of AI Table.

Variable	Min	Max	Number of values
Pressure, bar	10.6	250	15

Temperature, K	600	1208	21
Equivalence ratio, Φ	0.2	2.0	13
Residual content, xr	0.001	0.6	11

Interestingly, Table 3 highlights that the range of independent variables is properly selected to fit the hydrogen engine application, covering most of the thermodynamic conditions experienced in the unburned gas of the cylinder.
A knock event is recognized when the AI integral, expressed by Equation (3), exceeds a tunable threshold level which is considered lower than the unity.

$$\int \frac{dt}{\tau_{AI}} < Threshold = 0.85 \qquad (3)$$

The in-cylinder heat transfer (gas-to-wall) is replicated by a user sub-model resembling the Hohenberg equation. No particular refinement is adopted for intake and exhaust pipes, assigning reliable wall temperatures to the overall sub-systems.
NOx is reproduced by a multi-zone approach for the burned zone. The kinetic of NO is evaluated by applying the extended Zeldovich mechanism. Therefore, thermal NO emissions are computed, neglecting the other source terms.

Finally, a refined model for the estimation of unburned fuel is adopted, considering the filling/emptying of the crevices, the flame wall quenching, and the fuel post-oxidation [36]. The cylinder model is coupled with additional volumes, one that schematizes the piston crevice region, and a second additional crevice volume, positioned above the dead volume. According to a simple filling and emptying approach, the mass and energy fluxes exchanged between the cylinder and crevice volumes are computed. To estimate the amount of fuel that escaped from the combustion because of the flame extinction at the cylinder walls, the quenching distance is computed by the correlation in [37]. The unburned fuel still present in the cylinder at the combustion end is finally assumed to post-oxidize based on a tabulated kinetic approach.

6. Results Discussion

This section presents the numerical results obtained by the proposed simulation methodology applied to the examined engine. First, a focus will be dedicated to the in-cylinder turbulence and combustion characteristics; in the second stage, the computed performance and emissions of the hydrogen SI engine will be discussed.

6.1. Turbulence and Combustion

As known, the proper simulation of the turbulence process plays a relevant role in the subsequent prediction of combustion evolution in Spark Ignition engines. Indeed, the first step of the employed simulation methodology involves the in-cylinder turbulence phenomenon through the assessment of 1D outcomes with respect to 3D ones. In particular, the reliability of the 0D turbulence sub-model is tested assuming the target 3D data referred to the mass averages of mean flow velocity, turbulence intensity, and integral length scale deriving from motored simulations at a speed of 1700 rpm. A tuning procedure is adopted [29] to identify a unique set of tuning constants for the 0D turbulence sub-model, capable to reach a satisfactory matching with 3D findings. An adequate agreement is obtained on the main turbulence parameters, as depicted in Figure 2.
The overall 0D sub-model behaviour can be considered satisfactory for the integral length scale and the turbulence intensity along the intake and compression phases and the first part of the expansion

stroke. As for the mean flow velocity evolution, the 0D turbulence model shows a lower accuracy in reproducing the 3D flow decay occurring from the second stage of the intake process. Despite this drawback, the 0D sub-model is capable to forecast a flow velocity trend that resembles the one computed by the 3D model. For completeness, Figure 3 shows the mean flow velocity and the turbulent kinetic energy fields provided by the 3D analysis during the intake phase. From these plots, it is possible to appreciate that the turbulence intensity and flow velocity peaks reported in Figure 2b-c at -270 CAD ACTDC can be related to the presence of high-speed gas jets through the intake valve. The decay of high-speed gas jets according to the energy cascade mechanism leads to increased turbulent kinetic energy.

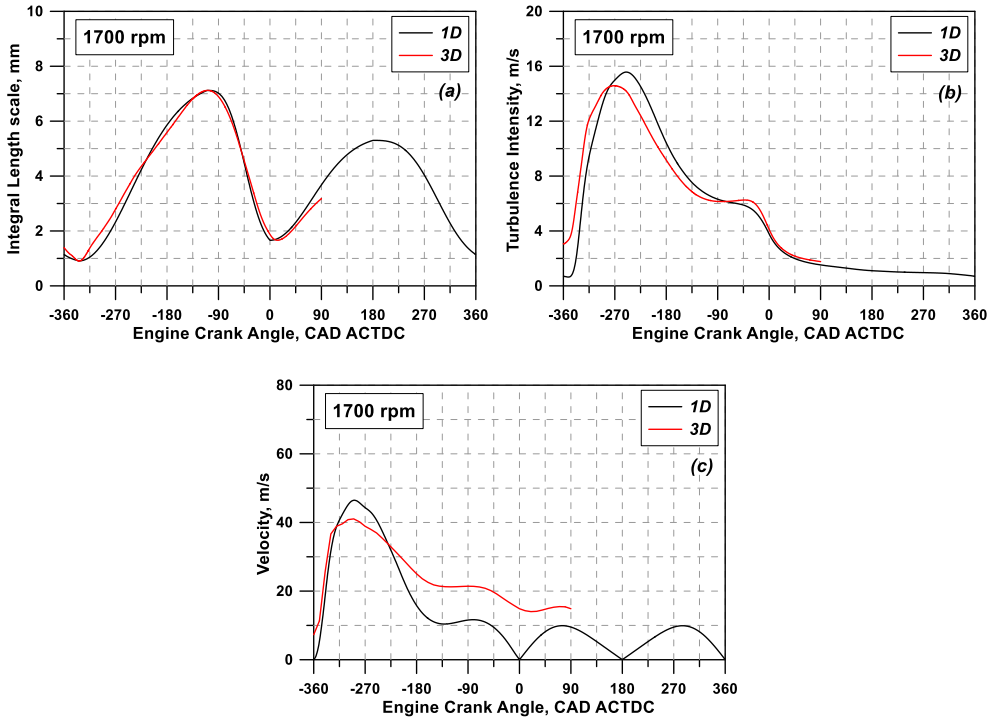

Figure 2. 1D/3D comparison of Integral length scale (a), turbulence intensity (b), and mean flow velocity (c) under motored conditions at a revving speed of 1700 rpm.

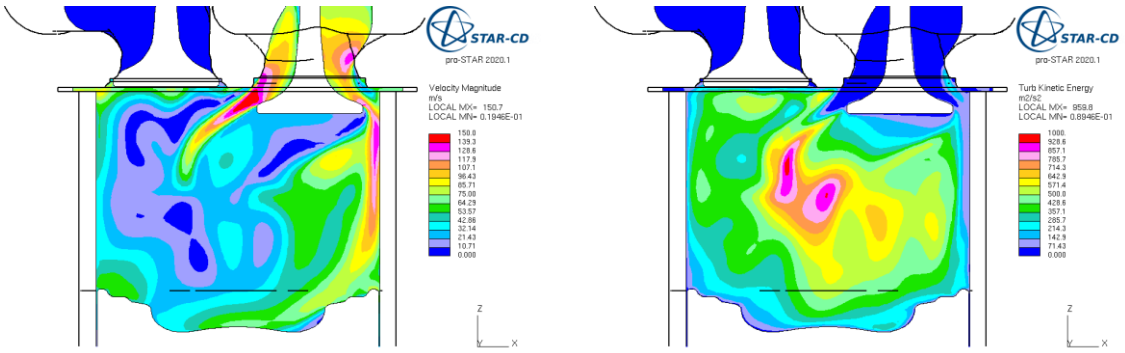

(a) (b)

Figure 3. Mean flow velocity (a) and turbulent kinetic energy (b) at -270 CAD ACTDC provided by the 3D model at 1700 rpm.

The second step of the simulation methodology regards the combustion, where the fractal combustion sub-model is calibrated against the 3D CFD result at a high load and 1700 rpm, with an ultra-lean mixture. After a simple tuning of the 0D sub-model, a quite satisfactory agreement is reached in terms of in-cylinder pressure evolution as depicted in Figure 4a. As visible, only limited deviations between 1D and 3D pressure traces are detected in the relevant combustion window, thus demonstrating the model ability in capturing the combustion under ultra-lean hydrogen/air mixture conditions. Moreover, both 1D and 3D codes concur in predicting the operation as knock-safe.
The procedure is further assessed by comparing the cylinder-out NO emissions based on 1D and 3D modelling approaches. NO emission furnished by the calibrated 1D model shows a satisfactory alignment with the respect to the related 3D outcome. Indeed, in the considered point (Figure 4b), a prediction error of 5.6% between the 3D-reference and 1D model is realized.

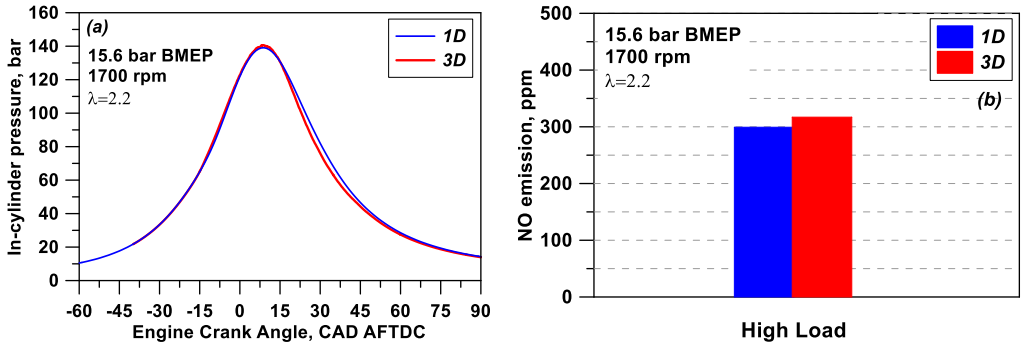

Figure 4. 1D/3D comparison of in-cylinder pressure traces (a) and NO emissions (b) for the 1700@15,6 case.

Besides the calibration purposes described above, the 3D model can be proficiently used to deepen the phenomena taking place inside the combustion chamber, such as nitrogen oxide (NO) formation. Figure 5a shows the flame front position, while Figure 5b reports the NO concentration at 10 CAD ATDC. It is possible to notice that NO formation takes place in the burned region where the highest gas temperatures are achieved. In particular, NO formation is stronger in the combustion chamber core.

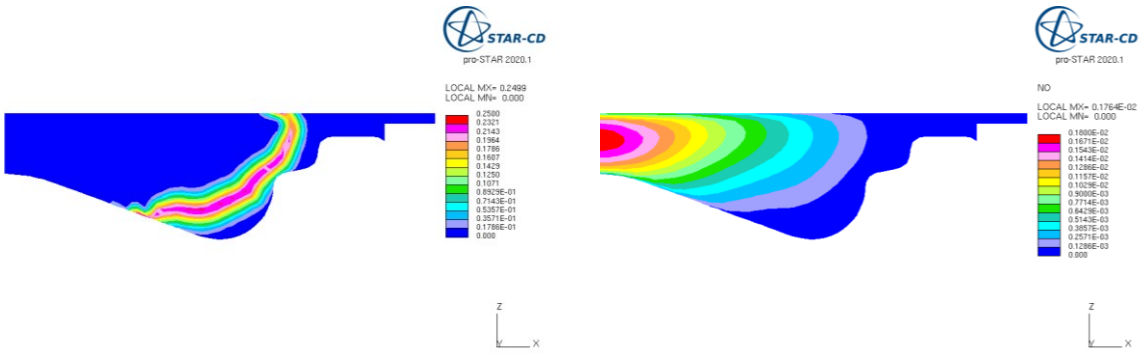

(a) (b)

Figure 5. Flame front position (a) and NO concentration (b) provided by the 3D simulation for the 1700@15,6 case at 10 CAD ATDC. As for the flame front, the proposed scalar field represents c·(1-c), where c is the progress variable.

Once the 1D model for the hydrogen SI engine is tuned against the 3D outcomes, it is utilized in a predictive way to provide the performance at the same operations as the Diesel engine. In this regard, a unique set of tuning constants both for turbulence and combustion sub-models is considered at varying operating conditions.

6.2. Performance and Emissions

In this section, the 1D numerical results of the hydrogen Spark Ignition engine are compared to the simulated outcomes of the Diesel engine, in terms of global performance parameters and NO emissions.

The performance assessment between the hydrogen SI engine and the Diesel one is carried out considering the same brake torque output.

Figure 6a reports the comparisons for the Gross indicated efficiency. The selection of this parameter instead of the brake efficiency derives from the need to exclude the variations of the pumping work for the case of engine exhaust at ambient pressure, as the one here considered. In Figure 6a, the converted hydrogen engine running under an ultra-lean mixture (relative air/fuel ratio, λ=2.2) exhibits similar or slightly lower levels of gross indicated efficiency with respect to the Diesel unit (average percent variations of ~2.5%). Based on the adopted tabulated knock approach, the converted hydrogen engine does not present knock issues at the analyzed operating points and mixture conditions. From a combustion perspective, the employment of a very-lean mixture for hydrogen combustion combined with a relatively low in-cylinder turbulence level of the donator engine involves certain penalizations in the burning duration and, consequently, in the thermodynamic efficiency. Despite the mixture leaning up to λ=2.2, the flame velocity of hydrogen allows for preserving the combustion stability, as well. It is worth underlying that these efficiency results are obtained from a net conversion of the original Diesel engine without any further modification or optimization.

Figure 6b shows the comparison of the cylinder-out NO emissions. It can be noted that a strong decrease in NO emissions for hydrogen engine with respect to the Diesel configuration is obtained, reaching a percent average reduction of ~67%. Indeed, the possibility to explore high levels of mixture dilution for hydrogen combustions allows for reducing the in-cylinder temperature peaks in the burned regions, thus lowering the generation of NO emissions.

At the same brake torque output, the combination of poor volumetric efficiency for a port hydrogen injection (due to low density of gaseous H_2) with the highly lean operation generates greater values of the intake plenum pressure with respect to the Diesel engine (Figure 7a). These results suggest the need for the design of an enhanced turbocharging system when the original engine is converted into a hydrogen SI unit, especially at increasing the load, the speed, and the mixture leaning.

The higher plenum pressure induces the rise of the in-cylinder pressure peaks. Indeed, Figure 7b shows that the hydrogen SI engine presents a general increase of the in-cylinder pressure peaks, reaching a maximum value equal to ~160 bar at 1800 rpm and 17.4 bar BMEP. This implies an intensification of the mechanical stress for the engine cylinders to be monitored to avoid mechanical failures

As already discussed above, the employment of a very lean hydrogen/air mixture leads, on the one hand, to a less efficient SI combustion process but, on the other hand, to some advantages such as heat transfer reduction. For instance, Figure 8a proposes the comparisons of the heat transfer on total fuel energy between Diesel and hydrogen SI variants. At the available speed/load points, the switching from the Diesel operation to the hydrogen one provides some benefits in terms of in-cylinder heat transfer, due to the lower in-cylinder gas temperatures. As expected, Figure 8a shows an enhanced impact of the heat transfer as the load decreases, and maximum heat transfer benefits equal to 2.5% are achieved at 1600@13.4 when the hydrogen SI combustion is realized. However, these advantages are still too low to substantially contribute to the efficiency improvements of the hydrogen SI engine with respect to the Diesel variant under medium/high loads.

Concerning the exhaust gas temperature, Figure 8b shows that the hydrogen SI engine, operating with a relative air/fuel ratio λ=2.2, exhibits temperature levels quite similar to the ones of the donator engine at the examined points.
In addition, it is expected that moving towards lower load regions and employing larger mixture dilution (above λ=2.2 and up to the combustion stability limit), decreased exhaust gas temperatures and further heat transfer reductions can be realized.

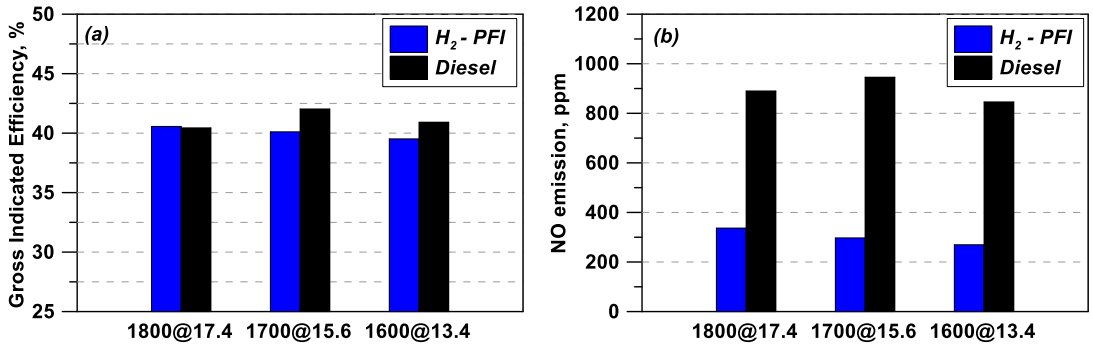

Figure 6. Comparison of Gross Indicated efficiency (a) and NO emissions (b), for hydrogen and Diesel operations.

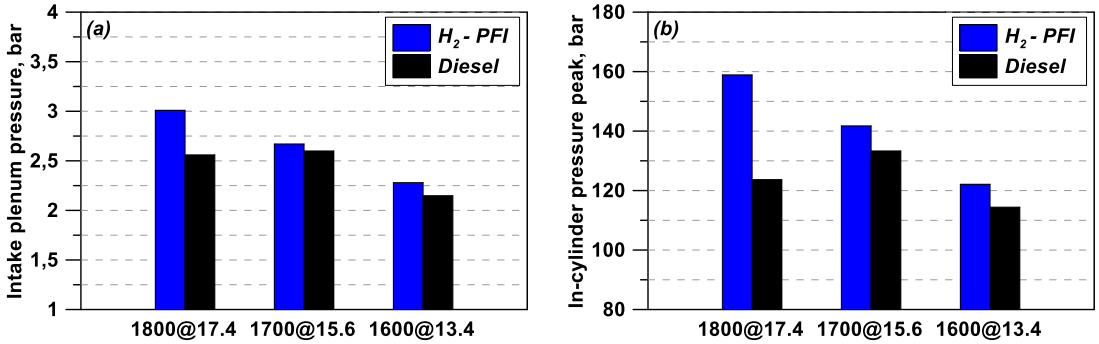

Figure 7. Comparison of intake plenum pressure (a) and in-cylinder pressure peak (b) for hydrogen and Diesel operations.

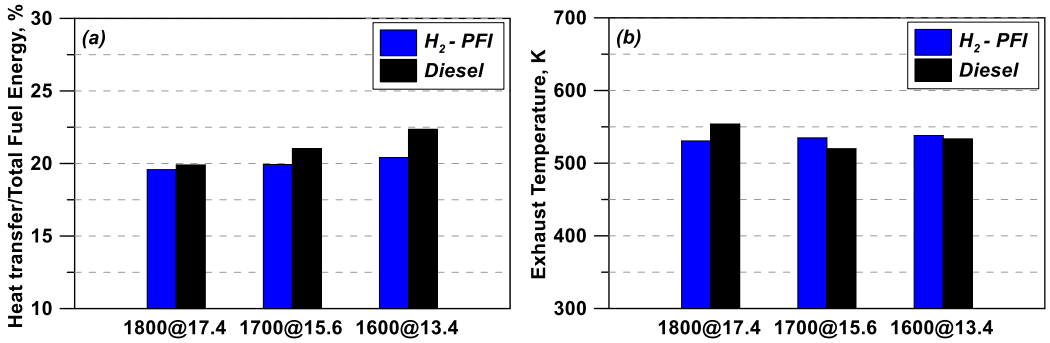

Figure 8. Comparison of in-cylinder heat transfer/total fuel energy (a) and engine exhaust temperature (b) for hydrogen and Diesel operations.

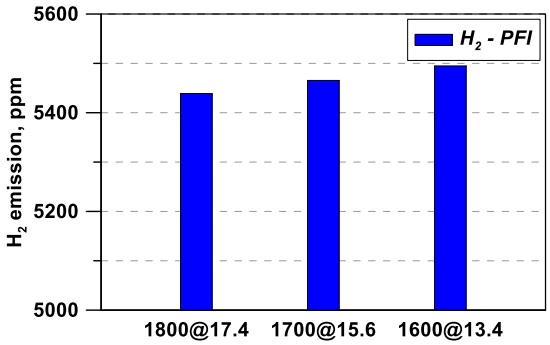

Figure 9. Modeled global unburned Hydrogen.

As an additional output of the 1D model, Figure 9 reports the bar chart of the unburned fuel concentration for the investigated operating conditions. Those emissions take into account the contributions of the above-mentioned related sources, namely the top land crevices, the additional crevice, and the flame-wall quenching. Because of the slight load variation, the unburned hydrogen values between the cases are quite similar, varying by about 100 ppm over 5500 ppm. The values here reported for the unburned H_2, are comparable to the level found in the current literature [38], [39]. Concerning the splitting of the sources, around 41% of the total ppm amount is due to the top land crevices, 31% to the additional crevice, and finally 26% to the quenching contribution.
Summarizing, the present numerical study highlights that a simple conversion of a donator Diesel engine into a port-injected hydrogen SI unit allows to drastically reduce the NO emissions with similar or slightly reduced gross indicated efficiency levels while delivering the same engine brake torque.
In a future research activity, a more refined numerical analysis for the hydrogen SI engine will be addressed, considering an advanced optimization of the control parameters to improve both efficiency and NO emissions. In addition, the adoption of some hardware modifications, including increased compression ratio, direct-injection configuration, or a re-design of intake ports, would allow to further enhance the combustion process and the performance of the engine.

7. Conclusion

In this work, a single cylinder Diesel engine is virtually converted into a hydrogen Spark Ignition unit, operating under ultra-lean mixture conditions, with the aim to forecast performance and emission variations. First, a Diesel engine is tested at steady conditions at medium/high loads, collecting the main performance and the in-cylinder pressure traces. A complete 1D model of the Diesel engine is developed in GT-Power and validated against the measurements, showing a satisfactory agreement. The conversion of the Diesel engine to a Spark Ignition version is supported by a 1D/3D simulation methodology, where 3D outcomes in terms of turbulence intensity and in-cylinder pressure cycle are taken as a reference to tune 0D turbulence and combustion sub-models implemented in the 1D code. In particular, the 1D combustion model is calibrated at a high load, 1700 rpm, and under an ultra-lean hydrogen/air mixture (λ=2.2). Once properly validated, the 1D model is applied to forecast the performance and emissions of the hydrogen SI engine. The main results of this numerical analysis can be summarized as follows:

- The conversion from a Diesel engine to a hydrogen Spark Ignition unit with the same brake torque output allows for preserving similar levels of the Gross Indicated efficiency; only limited efficiency reductions (an average penalization of 2.5%) for the examined points are detected;

- The hydrogen SI engine capable to preserve the same brake torque as the donator Diesel engine requires slightly higher boosting; this induces greater in-cylinder pressure peaks up to a maximum variation of 28% for the point at high speed and load (1800@17.4); despite the increase of pressure, hydrogen engine operations are knock-safe;
- The hydrogen SI engine operating with a relative air/fuel ratio of 2.2 generates strong reductions of the cylinder-out NO emissions with respect to Diesel operation, reaching a mean decrease of about 67%;
- A prediction of the unburned fuel emission has been estimated, demonstrating to show values similar to the ones reported in the current literature.

Finally, the validated simulation procedure can support and address the development phase of hydrogen Spark Ignition engines, providing the opportunity to numerically explore various engine architectures and combustion concepts and to optimize both performances, noxious and unburned fuel emission.

References

[1] Seungmoook O.H. et al., "Experimental Investigation of the hydrogen-rich offgas spark ignition engine under various compression ratios", Energy Conversion and Management, Volume 201, December, N. 112136. doi: 10.1016/j.enconman.2019.112136.

[2] Dhyani V. and Subramanian K.A., "Fundamental characterization of backfire in a hydrogen fuelled spark ignition engine using CFD and experiments", International Journal of hydrogen Energy, 44 no. 6, 2019: 32254-32270; https://doi.org/10.1016/j.ijhydene.2019.10.077.

[3] Pauer, T., Weller, H., Schunemann, E., Eichlseder, H. et al., "H2 ICE for Future Passenger Cars and Light Commercial Vehicles," in 41th International Vienna Motor Symposium, Vienna, 2020.

[4] MAN and Shell, "Shell, MAN and Connexxion Planning Worlds Largest Hydrogen Public Transport Project," in Green Car Congress, 2006, https://www.greencarcongress.com/2006/06/shell_man_and_c.html, accessed 02 Dec. 2021.

[5] Pauer, T., Weller, H., Schunemann, E., Eichlseder, H. et al., "H2 ICE for Future Passenger Cars and Light Commercial Vehicles," in 41th International Vienna Motor Symposium, Vienna, 2020.

[6] Saravanan, N., Nagarajan, G., Sanjay, G., Dhanasekaran, C. et al., "Combustion Analysis on a DI Diesel Engine with Hydrogen in Dual Fuel Mode," Fuel 87, no. 17-18 (2008): 3591-3599, doi: 10.1016/j.fuel.2008.07.011.

[7] Navale J.S. et al., "An experimental study on performance, emission and combustion parameters of hydrogen fueled spark ignition engine with the timed manifold injection system",

[8] Ganesh R.H. et al., "Hydrogen fueled spark ignition engine with electronically controlled manifold injection: An experimental study", Renewable Energy 33, Issue 6, pp. 1324-1333, 2008. Doi: 10.1016/j.renene.2007.07.003.

[9] Millo F. et al. Synergetic Application of Zero-, One-, and Three-Dimensional Fluid-dynamics Approaches for Hydrogen-fuelled Spark-Ignition engine simulation", SAE International Journal of Engines, Volume 15, Issue 4, 2022. Doi: 10.4271/03-15-04-0030.

[10] Keplatz. et al., "Loss Analysis of a Direct-Injection Hydrogen Combustion Engine," SAE Technical Paper 2018-01-1686, 2018, doi: 10.4271/2018-01-1686.

[11] Scarcelli R., Wallner, T., Obermair, H., Salazar, V.M. et al., "CFD and Optical Investigations of Fluid Dynamics and Mixture Formation in a DI-H2ICE," in ASME 2010 Internal Combustion Engine Division Fall Technical Conference, San Antonio, TX, 2010, doi:10.1115/ICEF2010-35084.

[12] Wallner T. et al., "Influence of Injection Strategy in a High-Efficiency Hydrogen Direct Injection Engine," SAE Int. J. Fuels Lubr. 5, no. 1 (2012): 289-300, doi: 10.4271/2011-01-2001.

[13] Berni F, Cicalese G, Sparacino S and Cantore G. On the existence of universal wall functions in in-cylinder simulations using a low-Reynolds RANS turbulence model. AIP Conf Proc 2019; 2191(1): 020019.
[14] Berni F and Fontanesi S. A 3D-CFD methodology to investigate boundary layers and assess the applicability of wall functions in actual industrial problems: A focus on in-cylinder simulations. Appl Therm Eng 2020; 174: 115320.
[15] Berni F, Cicalese G, Borghi M and Fontanesi S. Towards grid-independent 3D-CFD wall-function-based heat transfer models for complex industrial flows with focus on in-cylinder simulations. Appl Therm Eng 2021; 190: 116838.
[16] Cicalese, G., Berni, F., Fontanesi, S., D'Adamo, A., Andreoli, E. A Comprehensive CFD-CHT Methodology for the Characterization of a Diesel Engine: From the Heat Transfer Prediction to the Thermal Field Evaluation (2017) SAE Technical Papers, 2017-October, DOI: 10.4271/2017-01-2196.
[17] Berni, F., Cicalese, G., Fontanesi, S. A modified thermal wall function for the estimation of gas-to-wall heat fluxes in CFD in-cylinder simulations of high performance spark-ignition engines (2017) Applied Thermal Engineering, 115, pp. 1045-1062. DOI: 10.1016/j.applthermaleng.2017.01.055.
[18] Berni F, Sparacino S, Riccardi M, et al. A zonal secondary break-up model for 3D-CFD simulations of GDI sprays. Fuel 2022; 309: 122064.
[19] Senda J, et al. Modeling spray impingement considering fuel film formation on the wall. Warrendale, PA: SAE International, 1997.
[20] Habchi C. A comprehensive model for liquid film boiling in internal combustion engines. Oil Gas Sci Technol 2010; 65(2): 331–343.
[21] Colin O and Benkenida A. The 3-zones extended coherent flame model (Ecfm3z) for computing premixed/diffusion combustion. Oil Gas Sci Technol 2004; 59(6): 593–609.
[22] Bruneaux, G., T. Poinsot, and J.H. Ferziger, Premixed flame–wall interaction in a turbulent channel flow: budget for the flame surface density evolution equation and modelling. Journal of Fluid Mechanics, 1997. 349: p. 191-219.
[23] Y. Pei, M. Mehl, W. Liu, T. Lu, W. J. Pitz, and S. Som, "A Multi-Component Blend as a Diesel Fuel Surrogate for Compression Ignition Engine Applications," Journal of Engineering for Gas Turbines and Power, GTP-15-1057 (2015).
[24] Peters, N. Turbulent Combustion; Cambridge University Press: Cambridge, UK, 2000.
[25] Ewald, J.; Peters, N. On unsteady premixed turbulent burning velocity prediction in internal combustion engines. Proc. Combust. Inst. 2007, 31, 3051–3058.
[26] D'adamo, A., Iacovano, C., Fontanesi, S., A data-driven methodology for the simulation of turbulent flame speed across engine-relevant combustion regimes, 2021, Energies, vol. 14, DOI:10.3390/en14144210.
[27] D'Adamo, A., Breda, S., Iaccarino, S., Berni, F., Fontanesi, S., Zardin, B., Borghi, M., Irimescu, A., Merola, S. Development of a RANS-Based Knock Model to Infer the Knock Probability in a Research Spark-Ignition Engine (2017) SAE International Journal of Engines, 10 (3), DOI: 10.4271/2017-01-0551.
[28] Krishna Prasad Shrestha, Lars Seidel, Thomas Zeuch, Fabian Mauss. Detailed Kinetic Mechanism for the Oxidation of Ammonia Including the Formation and Reduction of Nitrogen Oxides. Energy & Fuels, American Chemical Society, 2018, 32 (10), pp.10202-10217. ff10.1021/acs.energyfuels.8b01056ff. ffhal-02629067.
[29] Bozza F. et al., "A refined 0D Turbulence model to predict tumble and turbulence in SI Engines", SAE International Journal of Engines, 12(1): 15-30, 2019. Doi: 10.4271/03-12-01-0002.
[30] Bozza F., et al., "Validation of a Fractal combustion model through flame imaging", SAE International Journal of Engines, Vol. 114, Section 3, pp. 973-987, 2005.
[31] Ranzi E. et al., "New reaction classes in the kinetic modeling of low temperature oxidation of n-

alkanes", Combustion and Flame 162, no. 5 1679-91 (2015). Doi: 10.1016/j.combustflame.2014.11.030.

[32] Teodosio L. et al., "Impact of the laminar flame speed correlation on the results of a quasi-dimensional combustion model for the Spark-Ignition engine", Energy Procedia, Vol. 148, Pages: 631-638, 2018. Doi: 10.1016/j.egypro.2018.08.151.

[33] Barbato A. et al., "A numerical exploration of engine combustion using toluene reference fuel and hydrogen mixtures", E3S Web of Conferences 321, 07003, 2021. Doi: 10.1051/e3sconf/202131207003.

[34] Bozza F. et al., "A Tabulated-Chemistry Approach Applied to a Quasi-Dimensional Combustion Model for a Fast and Accurate Knock Prediction in Spark-Ignition Engines," SAE Technical Paper 2019-01-0471, 2019, doi:10.4271/2019-01-0471.

[35] Hong Z. et al., "An improved H_2/O_2 mechanism based on recent shock tube/laser absorption measurements", Combustion and Flame 158(4): 633-644, 2011. Doi: 10.1016/j.combustflame.2010.10.002.

[36] Malfi E, De Bellis V, Bozza F, Cafari A, Caputo G, Hyvönen J. "A phenomenological model for the description of unburned hydrocarbons emission in ultra-lean engines", International Journal of Engine Research 23(6): 995-1011, 2022. Doi:10.1177/14680874211005063.

[37] Suckart, D., Linse, D., Schutting, E. et al. "Experimental and simulative investigation of flame–wall interactions and quenching in spark-ignition engines", Automotive Engine Technology 2: 25–38, 2017. Doi:10.1007/s41104-016-0015-z.

[38] Natkin, Robert J., et al. "Ford hydrogen engine laboratory testing facility", SAE Technical Paper, 2002-01-0241, 2002. Doi:10.4271/2002-01-02412002.

[39] Tsujimura, T., and Yasumasa S. "The utilization of hydrogen in hydrogen/diesel dual fuel engine", International journal of hydrogen energy 42.19:14019-14029, 2017. Doi:10.1016/j.ijhydene.2017.01.152.